Food Bioscience 80 (2026) 108969

Contents lists available at ScienceDirect

Food Bioscience

journal homepage: www.elsevier.com/locate/fbio

Linking integrative omics-based data fusion to *in vitro* gastrointestinal digestion reveals ripening-driven chemical signatures in Coppa Piacentina PDO

Federico Froldi [a,1], Gabriele Rocchetti [a,*,1], Giulia Leni [b], Gianluca Giuberti [b], Samantha Sigolo [a], Aldo Prandini [a]

[a] Department of Animal Science, Food and Nutrition, Università Cattolica Del Sacro Cuore, Via Emilia Parmense 84, 29122 Piacenza, Italy
[b] Department for Sustainable Food Process, Università Cattolica Del Sacro Cuore, Via Emilia Parmense 84, 29122 Piacenza, Italy

ARTICLE INFO

Keywords:
mixOmics
Metabolomics
INFOGEST
Bioaccessibility
Meat quality

ABSTRACT

Dry-cured meat ripening drives complex biochemical transformations that shape both product identity and gastrointestinal behaviour. In this study, an integrative strategy was applied to investigate how ripening-driven chemical organisation of Coppa Piacentina Protected Designation of Origin (PDO) influences its gastrointestinal metabolic outcome. Previously generated metabolomic, lipidomic and volatilomic datasets obtained from undigested samples at different ripening stages (fresh, 60, 90, 180 and 240 days) were integrated using a data fusion framework to obtain a system-level description of ripening-associated chemical signatures. Samples from the same ripening stages (n = 3) were subjected to the standardized INFOGEST *in vitro* digestion protocol, and intestinal digested samples were characterized by untargeted metabolomics using ultra-high-performance liquid chromatography coupled with high-resolution mass spectrometry (UHPLC-HRMS) together with free amino acid profiling. The untargeted analysis allowed the putative annotation of 1298 mass features mainly belonging to amino acids, peptides and lipid-related metabolites. Data fusion revealed coordinated molecular networks associated with ripening, highlighting proteolysis, lipid remodelling and oxidative processes. These ripening-driven signatures were not erased during digestion but translated into distinct intestinal metabolomic profiles. Short ripening induced moderate changes in bioaccessible metabolites, whereas prolonged ripening amplified digestive complexity, promoting the release of peptide derivatives and lipid-related metabolites without increasing total free amino acid release. Notably, selected γ-glutamyl peptides showed relative resistance to gastrointestinal degradation. These findings indicate that ripening acts as a system-level biochemical driver shaping both product composition and the metabolite profile generated during digestion.

1. Introduction

Dry-cured meat products are central to the culinary heritage of many countries and are increasingly recognized not only for their sensory and cultural value but also for their highly complex biochemical composition (Mediani et al., 2022). The ripening process of these products involves prolonged enzymatic and microbiological activities, resulting in profound and coordinated modifications of the proteome, lipidome, and metabolome (Rocchetti et al., 2023, 2025; Rutigliano et al., 2023). These transformations lead to the accumulation of a wide range of low molecular weight compounds, including peptides, free amino acids, fatty acids, and volatile metabolites, which collectively define the chemical identity and functional properties of the final product. Capturing this complexity requires integrative analytical strategies capable of moving beyond single-platform analyses toward a system-level interpretation of ripening-driven biochemical trajectories. In this context, metabolomics-based data fusion approaches have emerged as powerful tools to integrate complementary analytical windows of the metabolome (Becchi et al., 2025; Tomas et al., 2024), including untargeted metabolomics, lipidomics, and volatilomics. By enabling the simultaneous interpretation of multiple metabolomic datasets, data fusion strategies allow the identification of coordinated

* Corresponding author.
E-mail address: gabriele.rocchetti@unicatt.it (G. Rocchetti).
[1] These authors equally contributed to the work.

https://doi.org/10.1016/j.fbio.2026.108969
Received 12 January 2026; Received in revised form 3 April 2026; Accepted 22 April 2026
Available online 22 April 2026

molecular patterns and cross-platform correlations associated with food processing, providing a more comprehensive description of biochemical changes than isolated omics approaches.

Among Italy's most renowned dry-cured products, Coppa Piacentina Protected Designation of Origin (PDO) stands out for its distinctive production protocol and extended ripening potential. Produced from selected pork neck muscles, this cured meat undergoes a slow ripening process that may last up to 240 days or longer, during which endogenous and microbial enzymes drive intense proteolysis and lipolysis. Although the sensory, physicochemical, and compositional evolution of dry-cured meats during ripening has been extensively investigated (Martín-Miguélez et al., 2024; Sirtori et al., 2020), the integrated chemical signatures emerging from the interaction of different metabolite classes remain insufficiently explored.

Beyond product characterization, increasing attention has been directed toward understanding how ripening-induced biochemical modifications influence food behaviour under gastrointestinal conditions. *In vitro* digestion models are not intended to replace *in vivo* evidence, but rather to provide a mechanistic and reproducible framework to investigate how processing-driven molecular changes translate into digestive behaviour. In this regard, several studies have demonstrated that proteolysis- and lipolysis-related transformations occurring during ripening can substantially modulate the release, stability, and accessibility of nutrients and bioactive compounds during digestion (Egger et al., 2016; Gallego et al., 2017; Izquierdo-Sandoval et al., 2024; Tormási et al., 2025). The INFOGEST static *in vitro* digestion model has emerged as a consensus protocol to simulate oral, gastric, and intestinal phases of human digestion, facilitating inter-study comparability and supporting nutritional and mechanistic investigations (Egger et al., 2016). When coupled with untargeted high-resolution metabolomics based on UHPLC-HRMS, this approach enables detailed characterization of the molecular transformations occurring during digestion and supports the identification of digestion-derived metabolites potentially relevant to nutrient bioaccessibility and biological activity (Izquierdo-Sandoval et al., 2024; Rocchetti et al., 2024a, 2024b; Tormási et al., 2025).

In the present study, we applied an integrated experimental strategy to investigate the impact of ripening on Coppa Piacentina PDO at both the product and digestive levels. Metabolomic, lipidomic, and volatilomic datasets of undigested samples collected at different ripening stages (fresh, 60, 90, 180, and 240 days) were integrated using a multivariate data fusion approach to elucidate coordinated chemical changes associated with ripening. In parallel, samples from the same ripening stages were subjected to *in vitro* gastrointestinal digestion according to the INFOGEST protocol, and intestinal digested samples were characterized by untargeted UHPLC-HRMS metabolomics and free amino acid profiling. The aim of this study was to integrate multi-omics datasets to obtain a system-level understanding of the biochemical evolution occurring during Coppa Piacentina PDO ripening and to evaluate how these ripening-driven chemical signatures are translated into the metabolomic landscape generated during gastrointestinal digestion. We hypothesized that ripening establishes coordinated molecular networks involving metabolites, lipids and volatile compounds, and that these integrated chemical signatures are not completely disrupted during digestion but instead influence the pool of metabolites released and potentially bioaccessible under gastrointestinal conditions. This approach seeks to bridge product-level chemistry with digestive transformation through an integrated metabolomics perspective.

2. Materials and methods

2.1. Collection of Coppa Piacentina PDO samples

Samples of Coppa Piacentina were obtained from a certified producer affiliated with the Salami Piacentini PDO Consortium. The experimental design included three biological replicates for each of the following ripening stages: 0 (fresh), 60, 90, 180, and 240 days. All products were manufactured in accordance with the specifications set out by Commission Regulation (EC) No 1263/96. The biological replicates originated from Duroc × Topigs TN70 pigs reared on the same farm and fed a cereal- and soybean meal-based diet, in compliance with the requirements of the Coppa Piacentina PDO specification. All samples were obtained from products manufactured under the PDO specification of Coppa Piacentina, ensuring standardized processing conditions and comparable ripening trajectories across biological replicates. At the raw stage (T0; fresh samples), the average weight of the samples was 3200 ± 105 g, with a dry matter (DM) content of 39% ± 3.9, measured following ISO 1442:1997. As ripening progressed, the dry matter content increased as follows: 50% ± 2.8 at 60 days, 54% ± 6.5 at 90 days, 64% ± 4.2 at 180 days, and 68% ± 3.0 at 240 days. The mean weight of the ripened products was 2130 ± 384 g. Upon arrival, all samples were vacuum-packed, maintained at 4 °C, then minced and stored at −20 °C until further analysis.

2.2. In vitro gastrointestinal digestion (INFOGEST)

All the Coppa Piacentina PDO samples underwent an *in vitro* digestion mimicking human gastro-intestinal conditions by following the standardized INFOGEST static protocol, as described by Brodkorb et al. (2019). The *in vitro* digestion method involves the exposure of the food to three successive digestive phases: oral, gastric and intestinal. The oral phase was simulated by the use of simulated salivary fluid plus human salivary amylase at 75 U/mL (A1031; Merck KGaA, Darmstadt, Germany) the gastric phase by mixing simulated gastric fluid plus pepsin (P7012; Merck KGaA, Darmstadt, Germany) and a rabbit gastric extract (RGE70; Lipolytech S.A., Marseille, France), at 2000 and 60 U/mL, respectively, and the intestinal phase by using simulated intestinal fluid plus bile salts (B8631; Merck KGaA, Darmstadt, Germany) at 10 mM and pancreatin (P7545; Merck KGaA, Darmstadt, Germany) with a trypsin activity of 100 U/mL. The experimental conditions for the digestion procedure, such as pH adjustments, timing, types and enzyme activities, were based on available physiological data as detailed and justified by Minekus et al. (2014) and by Brodkorb et al. (2019). All the *in vitro* conditions were scaled up considering 15 g for each sample. At the end of the *in vitro* digestion protocol, samples were centrifuged (i.e., 6000×*g* for 20 min at 4 °C) and the liquid aliquots were collected and stored at −18 °C until further analysis.

2.3. Quantification of free amino acids during in vitro gastrointestinal digestion

The *in vitro* digested samples were then subjected to free amino acid analysis. Briefly, 100 μL of each digested samples was mixed with 30 μL of 5 mM norleucine (from Sigma-Aldrich), and the final volume was adjusted to 1 mL with Milli-Q water. Samples were then derivatised with 6-aminoquinolyl-*N*-hydroxysuccinimidyl carbamate and analyzed using an HPLC/ESI-MS system (Thermo-Fisher Scientific, San Jose, CA, USA), as previously described by Leni et al. (2024).

2.4. Untargeted profiling of small metabolites in digested samples by UHPLC-HRMS approach

Metabolomic profiling was done using a Vanquish UHPLC system (Thermo Scientific, Waltham, MA, USA) coupled to a heated electrospray ionization (HESI)-II source and a Q Exactive™ Focus Hybrid Quadrupole-Orbitrap Mass Spectrometer (Thermo Scientific, Waltham, MA, USA), using water and acetonitrile (Sigma-Aldrich, Milan, Italy) as the mobile phases, considering a gradient elution (from 6 up to 94% acetonitrile) in 35 min, with 0.1% formic acid as a phase modifier. The injection volume was 6 μL and ACQUITY CSH C18 Column (130 Å, 1.7 μm, 2.1 × 150 mm, from Waters) was used for chromatographic separation. The HRMS parameters were optimized from previously

published works by our research group (Rocchetti, Leni, et al., 2024). Shortly, the flow rate was set at 200 μL/min and full scan MS analysis was carried out in positive ionization mode with a mass resolution of 70, 000 at m/z 200, covering a range of 80-1200 m/z. The automatic gain control target (AGC target) was set to $1e^6$, and the maximum injection time (IT) was set to 200 ms. To acquire data-dependent (Top N = 3) MS/MS spectra, randomized injections of pooled quality control (QC) samples were performed, with the full scan mass resolution set at 17, 500 at m/z 200. The AGC target value was adjusted to $1e^5$, maximum injection time (IT) was limited to 100 ms, and an isolation window of 1.0 m/z was applied. Fragmentation of the selected ions was achieved using normalized collisional energy (23.3 eV). The following HESI parameters were used for both MS and MS/MS analyses: sheath gas flow at 40 arb, auxiliary gas flow at 20 arb, spray voltage at 3.5 kV, and capillary temperature of 320 °C. Prior to data acquisition, the mass spectrometer was calibrated using Pierce™ positive ion calibration solution (Thermo Fisher Scientific, San Jose, CA, USA), ensuring accurate mass measurements. The raw data obtained from the HRMS analysis were then processed using the MS-DIAL software (version 4.90) (Tsugawa et al., 2015). The alignment of chemical features was performed through automatic peak finding after LOWESS normalization, and compound annotation was achieved by comparing the acquired spectra with the FooDB ESI-POS library (version 1.0). Also, raw data were corrected against the *in vitro* digestion blank (only enzymes). The mass range 80-1200 m/z was explored to identify features with a minimum peak height of 10,000 cps. Peak centroiding for MS and MS/MS was performed with a tolerance of 0.05 and 0.1 Da, respectively. Retention time information was not considered in the calculation of the total score. The putative annotation step was based on criteria including mass accuracy, isotopic pattern, and spectral matching, which were employed to calculate a comprehensive library match score for each feature. The threshold value for the library match score was >50%, considering the most relevant ESI positive adducts. Gap filling was carried out using the peak finder algorithm to include missing peaks, with a tolerance of 5 ppm for m/z values. The reproducibility was evaluated by calculating the Relative Standard Deviation (RSD %) of each annotated metabolite in the randomly injected pooled QC sample (Ghosh et al., 2021). A level 2 of confidence in identification (i.e., putatively annotated compounds, i.e. MSI level 2) was achieved (Blaženović et al., 2018).

2.5. Multivariate and data fusion analysis

In this study, metabolomics, lipidomics and volatilomics data were integrated to obtain a comprehensive view of the biochemical processes underlying the ripening of Coppa Piacentina PDO. All omics layers were generated from the same physical batches of Coppa Piacentina PDO samples used in our previous studies (Leni et al., 2024; Rocchetti et al., 2023, 2025), where sample preparation, extraction procedures and instrumental conditions are fully described. Each analytical platform analyzed aliquots obtained from the same homogenized samples corresponding to the five ripening stages. QC pooled samples and analytical performance metrics (including RSD values) were previously reported in the original publications. Particularly, the three datasets previously generated and published by our research group, were reprocessed here using a new unified pipeline for integrative data fusion analysis. The integration of metabolomics, lipidomics and volatilomics datasets was performed using the Data Integration Analysis for Biomarker discovery using Latent variable approaches for Omics studies (DIABLO) framework implemented in the mixOmics package (version 6.26) in R software (version 4.4.1), as previously described by Becchi et al. (2025). This multiblock approach enables the identification of correlated molecular signatures across multiple omics datasets while simultaneously discriminating predefined biological groups. In the present study, DIABLO was applied to identify coordinated metabolite, lipid and volatile compound patterns associated with the different ripening stages of Coppa Piacentina PDO. Prior to modeling, each dataset was centered and scaled to unit variance. The DIABLO model was implemented as a multiblock sparse partial least squares discriminant analysis (block sPLS-DA) integrating the three omics layers. Model parameters were optimized using the tune.block.splsda function by testing different combinations of variables retained per block (keepX). Model performance was evaluated through repeated M-fold cross-validation (5 folds, 10 repeats), and the optimal configuration was selected based on the minimum overall error rate (i.e., 0.25). The final optimized model retained 10 discriminant variables per omic block for component 1, and 15 variables per block for component 2. Variable selection was embedded within the DIABLO modeling framework, ensuring that feature selection was performed within the cross-validation procedure. The selected variables represent the most discriminant and highly correlated features across the integrated omics layers contributing to the characterization of ripening-associated molecular signatures. For visualization purposes, the most contributing variables for each component were displayed using loading and contribution plots generated within the mixOmics environment. For *in vitro* digested samples, the multivariate data analysis of mass features was performed using the software MetaboAnalyst 6.0 (Pang et al., 2024). Briefly, data were median-centered, Pareto scaled, and Log_{10}-transformed before building unsupervised and supervised statistical models, namely hierarchical clustering (HCA), sparse Partial Least Squares Discriminant Analysis (sPLS-DA) and Orthogonal Projection to Latent Structures Discriminant Analysis (OPLS-DA), respectively. The performance of the sPLS-DA models was evaluated using a 5-fold cross-validation procedure. The OPLS-DA models were formerly built and validated considering the pairwise comparisons "T0 *vs* Short-Ripened (T60-T90)" and "T0 *vs* Long-Ripened (T180-T240), recording both goodness of fitting (R^2Y) and goodness of prediction (Q^2) parameters. Model robustness was further assessed by permutation testing (N = 100 permutations) implemented in MetaboAnalyst 6.0 to exclude overfitting. The importance of each compound for discrimination was evaluated using the variables importance in projection (VIP) selection method, using a VIP score threshold of >0.8. Further, a Volcano Plot analysis was carried out coupling Fold-Change (FC) analysis (cut-off >1.2) and one-way ANOVA ($P < 0.05$ with False Discovery Rate correction) to check the significant variation of metabolites in ripened samples against T0. Finally, to provide an additional measure of the magnitude of the observed differences, effect sizes were calculated in R software (version 4.4.1) for selected discriminant metabolites using Cohen's d together with their 95% confidence intervals, considering the comparisons Short-ripened vs T0 and Long-ripened vs T0.

3. Results and discussion

3.1. Correlation analysis reveals the cross-talk between metabolomic, lipidomic, and volatilomic layers on ripened samples

The DIABLO-based data fusion analysis enabled an integrative interpretation of metabolomic, lipidomic and volatilomic datasets, revealing a coordinated biochemical evolution of Coppa Piacentina PDO during ripening (Fig. 1). The projection of samples onto the first two latent components (Fig. 1A) showed a clear temporal structuring of the product, with component 1 discriminating the fresh product (T0) from all ripened samples and component 2 capturing progressive biochemical changes associated with prolonged ripening, particularly evident at 240 days (T240). The model showed strong agreement among the three omic layers, with very high pairwise correlations between metabolomics, lipidomics and volatilomics blocks. For component 1, correlation coefficients approached unity (i.e., 0.99–1.00), indicating that all analytical platforms captured the same dominant variance separating fresh and ripened samples. Similarly, component 2 displayed high cross-block correlations (i.e., 0.91–0.95), despite reflecting more subtle biochemical modifications occurring during advanced ripening stages. It should be

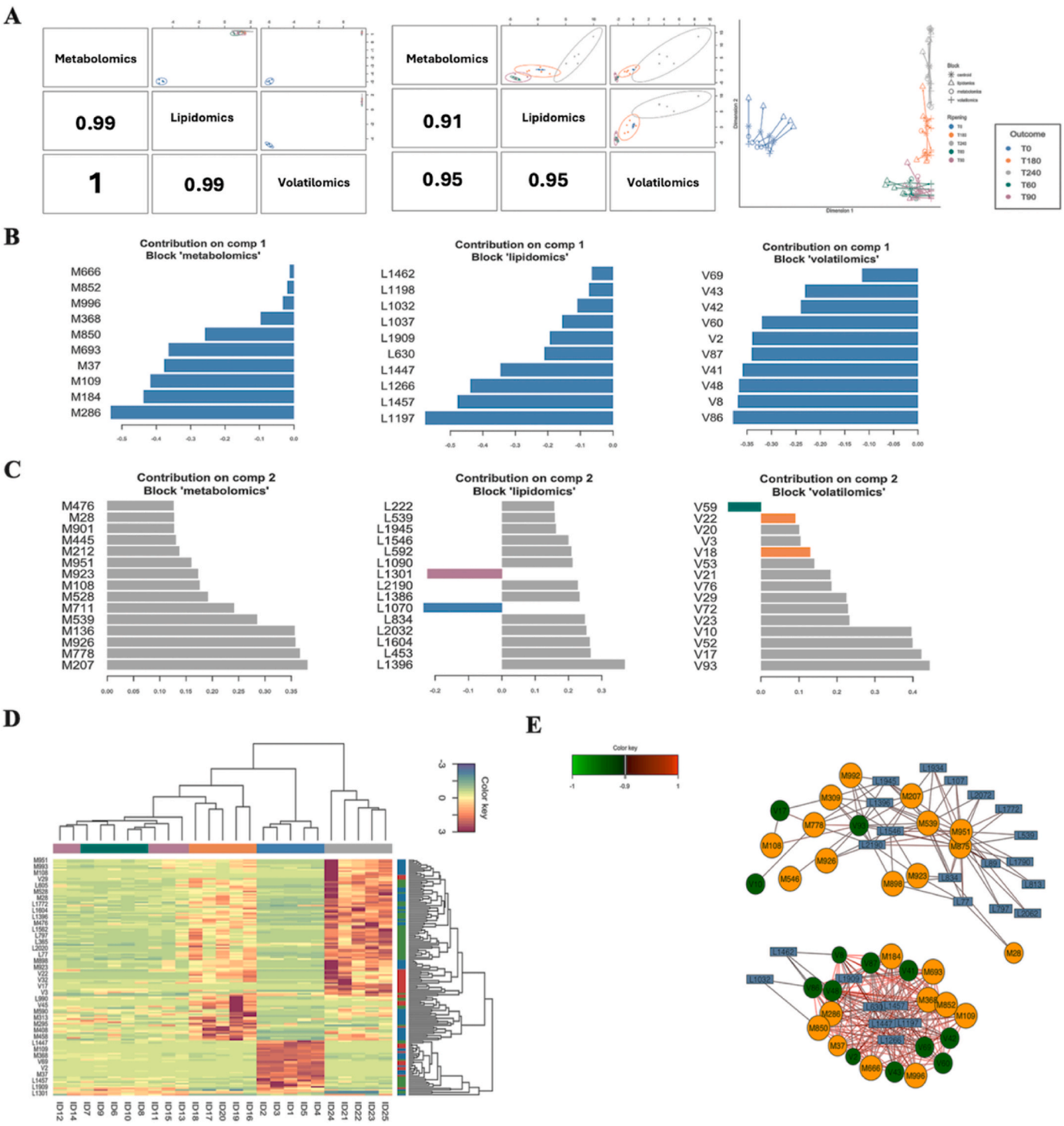

Fig. 1. DIABLO data fusion integration. A. Correlation matrices and arrow plot obtained by comparing the three blocks (metabolomics, volatilomics, lipidomics) involved in the components used for the DIABLO model (i.e., components 1 and 2). B-C. Loading score plots for top contributing variables per component 1 and 2 identified by the DIABLO model. D. Heatmap-based correlation plot for the variables selected by multiblock sPLS-DA performed. E. Correlation network for the variables selected by multiblock sPLS-DA performed (Orange color: metabolites; Blue color: lipids; green color: volatiles). Acronyms of metabolites, lipids, and volatiles are fully explained in supplementary material.

noted that these correlations refer to relationships between latent components extracted from each omics block rather than between individual variables. Because DIABLO maximizes covariance across datasets while discriminating predefined groups, very high cross-block correlations can occur when multiple omics layers capture coordinated biological processes.

The persistence of strong correlations across both components indicates that the biochemical processes governing Coppa Piacentina PDO ripening involve coordinated transformations across polar metabolites, complex lipids and volatile compounds rather than changes within a single chemical class. Importantly, the high concordance observed for component 2 suggests that prolonged ripening induces system-wide metabolic rearrangements rather than isolated biochemical events, as also reported in literature (Mu et al., 2026; Sugimoto et al.,

2020; Xun et al., 2026). The arrow plot further highlighted this agreement among analytical platforms, with metabolomics, lipidomics and volatilomics vectors showing similar orientations in the multivariate space. This convergence indicates that the different analytical windows captured common biochemical processes underlying ripening.

Component 1 therefore represented the main axis separating fresh and ripened Coppa Piacentina PDO (Fig. 1B). T0 samples clustered distinctly and were characterized by metabolites related to redox balance, primary amino acid metabolism and short-chain lipid species. In the metabolomic block, T0 was associated with peptides and amino acid-related compounds such as Pro-Pro-Phe, N-acetyl-L-alanine, cysteine-S-sulfate, glutathione and S-adenosyl-L-methionine, suggesting a metabolically active matrix still dominated by endogenous muscle components and antioxidant systems. The concomitant presence of acylcarnitines and furoyl derivatives further indicates early-stage lipid metabolism and the prevalence of Maillard-related precursors rather than advanced oxidative products (Fig. 1B and supplementary material). Consistently, the lipidomic block at T0 was enriched in phosphatidylcholines, lysophospholipids and sphingolipid species (e.g. PC 36:4, LPC 32:1, SM 35:7; 3O), reflecting the structural integrity of membrane-derived lipids in the fresh product. In parallel, the volatilomic profile of T0 was dominated by low-reactivity hydrocarbons and short-chain alcohols, indicative of limited secondary lipid oxidation (Fig. 1B and supplementary material). In contrast, component 2 (Fig. 1C and supplementary material) captured biochemical features associated with advanced ripening, with T240 samples clearly displaced along this axis across all omic layers. At the metabolomic level, long-ripened Coppa Piacentina PDO was characterized by γ-glutamyl peptides, Amadori-type compounds, oxidized fatty acid derivatives and complex lipid-related metabolites. The presence of hydroperoxy fatty acids, fructosylated amino acids and γ-glutamyl conjugates points to an interplay between proteolysis, lipid oxidation and secondary non-enzymatic reactions occurring during prolonged ripening (Domínguez et al., 2019). Lipidomic markers at T240 further supported this interpretation, with enrichment of ceramides, N-acyl amino acids and triglycerides containing highly unsaturated fatty acyl chains, reflecting membrane remodelling, lipolysis and cumulative oxidative stress (Domínguez et al., 2019). These transformations were mirrored by the volatilomic block, where aldehydes, ketones and unsaturated alcohols derived from lipid oxidation (e.g. hexanal, 2-heptenal, 2-octenal, 1-octen-3-ol) became prominent, contributing to the aromatic complexity of long-ripened samples (Fig. 1C and supplementary material), as also reported in literature (Zhang et al., 2019).

Hierarchical cluster analysis performed on the DIABLO-selected features (Fig. 1D) confirmed a clear stratification of samples according to ripening stage, driven by a restricted subset of highly discriminant markers rather than global compositional differences. This supports the concept that ripening-associated chemical fingerprints emerge from coordinated changes across multiple metabolite classes. A correlation network constructed using a stringent cut-off (Pearson's coefficients $\geq$0.9) further revealed dense connectivity between metabolites, lipids and volatile compounds (Fig. 1E and supplementary material). Redox- and amino acid-related metabolites such as glutathione, cysteine-S-sulfate, S-adenosyl-L-methionine, Pro-Pro-Phe and 2-furoylglycine emerged as highly connected hubs linking primary metabolism with lipid remodelling and volatile formation. Several phospholipids and N-acyl amino acid derivatives also displayed extensive correlations with polar metabolites and volatile oxidation products, highlighting their central role in the biochemical network modulated by ripening. Among the metabolites most strongly associated with the fresh Coppa Piacentina PDO (T0), S-adenosyl-L-methionine (SAM), 3-Hydroxy-11*Z*-octadecenoylcarnitine and cysteine-S-sulfate emerged as highly discriminant features (supplementary material), establishing numerous correlations with lipid and volatile compounds. The prominent loading of SAM on component 1 underscores its role as a marker of the initial biochemical state of the muscle matrix prior to ripening. SAM represents a central metabolic node (Yue et al., 2010), acting as the universal methyl-group donor in transmethylation reactions (Kempf et al., 2025) and playing a key role in amino acid metabolism, polyamine synthesis and redox homeostasis. Its association with T0 is consistent with a metabolically intact tissue, where endogenous enzymatic systems and one-carbon metabolism pathways are still preserved. As ripening progresses, the depletion of SAM likely reflects the combined effects of post-mortem metabolism, microbial activity and the gradual exhaustion of high-energy cofactors associated with living muscle tissue (Estévez et al., 2020). This decline aligns with the biochemical transition captured by DIABLO, in which the fresh product is characterized by redox-related metabolites and intact membrane lipids, whereas ripened samples display products of proteolysis, lipid remodelling and oxidative reactions. The role of SAM in the biosynthesis of biogenic amines has also been previously reported (Rocchetti et al., 2021; Tsafack & Tsopmo, 2022). However, considering the chemical lability of SAM, its decline during ripening should be interpreted as a putative indicator associated with the transition from fresh muscle metabolism to the cured product rather than as a direct mechanistic marker.

Overall, DIABLO captured metabolites that meaningfully reflect the temporal evolution of Coppa Piacentina PDO during ripening. The integrative analysis indicates that ripening is mainly driven by three interconnected biochemical processes: proteolysis and peptide metabolism, lipid remodelling and oxidation, and microbial-associated metabolic transformations. These findings support the suitability of integrative omics approaches to describe traditional meat products as dynamic biochemical systems in which ripening represents a progressive transformation from the metabolic architecture of fresh muscle to a mature cured product.

3.2. *Untargeted metabolomic profiling of Coppa Piacentina PDO digested samples*

While the DIABLO-based data fusion approach provided a system-level description of the coordinated chemical evolution of Coppa Piacentina PDO during ripening, these results primarily reflect the compositional and structural properties of the undigested product. However, the nutritional and biological relevance of such ripening-associated chemical fingerprints ultimately depends on their human gastrointestinal metabolic behaviour (Paolella et al., 2015). Indeed, many of the metabolites, lipids and reaction products identified as key drivers of ripening may undergo further transformation, degradation or selective release during digestion, thereby reshaping the molecular profile to which the host is actually exposed. In this context, the integrative product-level signatures obtained through data fusion (Fig. 1 and supplementary material) represent a necessary but not sufficient step to understand the functional implications of long ripening. To address this gap, the INFOGEST *in vitro* digestion model was applied to Coppa Piacentina PDO at different ripening stages in order to investigate how the coordinated biochemical networks identified in the undigested matrix are translated into the metabolomic landscape of the intestinal digestate. This combined approach was used to link ripening-driven chemical organisation at the product level with gastrointestinal transformation, providing a coherent framework to interpret digestibility and metabolic accessibility as a function of ripening time.

The untargeted metabolomic analysis on *in vitro* digested samples (based on UHPLC-HRMS) allowed the putative annotation of 1298 mass features. The putative annotation against the FooDB resulting in chemical classes mainly belonging to amino acids, peptides and analogues (184 compounds), followed by carbohydrate conjugates (69 compounds), and lipid molecules (including fatty acyl glycosides, fatty acid esters, and glycerophospholipids). A detailed list reporting all the annotated compounds is available as supplementary material, where each compound is indicated with its relative abundance value, adduct type, formula, INCHIKEY, SMILES, library match score, Signal-to-Noise ratio, MS1 isotopic spectrum, and MS/MS spectrum. In this work, only

the mass features presenting an RSD% value < 30% were considered for the following multivariate data analyses, thus supporting the robustness of our annotation strategy. Looking at the relative abundance values for the pooled QC samples, we found a great representativeness of several metabolites, mainly belonging to amino acids and derivatives, such as isoleucine, phenylalanine, methionine, tyrosine, and betaine (supplementary material). Additionally, 100 compounds were also structurally confirmed against the FooDB positive library, using the available MS/MS spectral information. Interestingly, the dataset of Coppa Piacentina PDO digested samples was also characterized by common metabolites previously outlined by DIABLO as main biomarkers of the undigested and ripened product, such as S-adenosyl-L-methionine, N-γ-L-Glutamyl-L-isoleucine, N-(1-Deoxy-1-fructosyl)leucine, Pro-Pro-Phe, and 2-Methylbenzoic acid (Supplementary Table 1).

As the first step, we carried out unsupervised and supervised statistical analyses to discriminate the different samples under investigation, and the results are showed in Fig. 2, considering on one side the heat map resulting from the hierarchical clustering approach (Fig. 2A) and on the other side the bidimensional score plot from sPLS-DA (Fig. 2B). The unsupervised hierarchical cluster analysis performed on the metabolomic profiles of intestinal digested samples revealed a clear separation between digested samples and the blank controls, confirming the effectiveness and reproducibility of the INFOGEST protocol (Fig. 2A). Digested Coppa Piacentina PDO samples clustered distinctly from the blank (only enzymes), indicating that the detected metabolic features originated predominantly from the food matrix rather than from enzymatic or buffer-related artefacts. Within the digested samples, a partial stratification according to ripening time was observed, suggesting that the extent of ripening modulated the composition of metabolites released during the intestinal phase. This trend was further confirmed by the supervised sPLS-DA model (Fig. 2B), which provided a clear discrimination between fresh and ripened digested samples along the first component (34.2% of explained variability), while the second component captured more subtle differences among ripening stages (10.6% of explained variability). Notably, samples corresponding to intermediate and advanced ripening times showed a tighter clustering compared to T0, indicating a progressive convergence of the intestinal metabolomic profile as ripening proceeded. These results suggest that ripening not only alters the undigested product composition, as highlighted by the data fusion analysis, but also reshapes the pool of metabolites that become bioaccessible during digestion. Overall, the multivariate structure observed in Fig. 2 indicates that the chemical organisation developed during ripening persists through *in vitro* gastrointestinal digestion and contributes to defining distinct intestinal metabolomic signatures.

3.3. Impact of ripening on the gastrointestinal behaviour of Coppa Piacentina metabolites

The *in vitro* digested samples were first subjected to amino acid analysis to evaluate the release of free amino acids during simulated gastrointestinal digestion. The total amount of free amino acids detected at the end of digestion is reported in the supplementary material. Total free amino acid concentrations ranged from 517 ± 59 mg/100 g in the 60 days-ripened samples to a maximum of 847 ± 119 mg/100 g in the fresh Coppa Piacentina PDO sample (supplementary material). Compared to the fresh product (T0), all ripened samples showed significantly lower ($P < 0.05$) levels of total free amino acids. This result suggests that, in ripened Coppa Piacentina PDO, gastrointestinal proteolysis may preferentially promote the formation and release of peptides rather than free amino acids. In agreement with this hypothesis, previous studies have reported that biochemical changes occurring

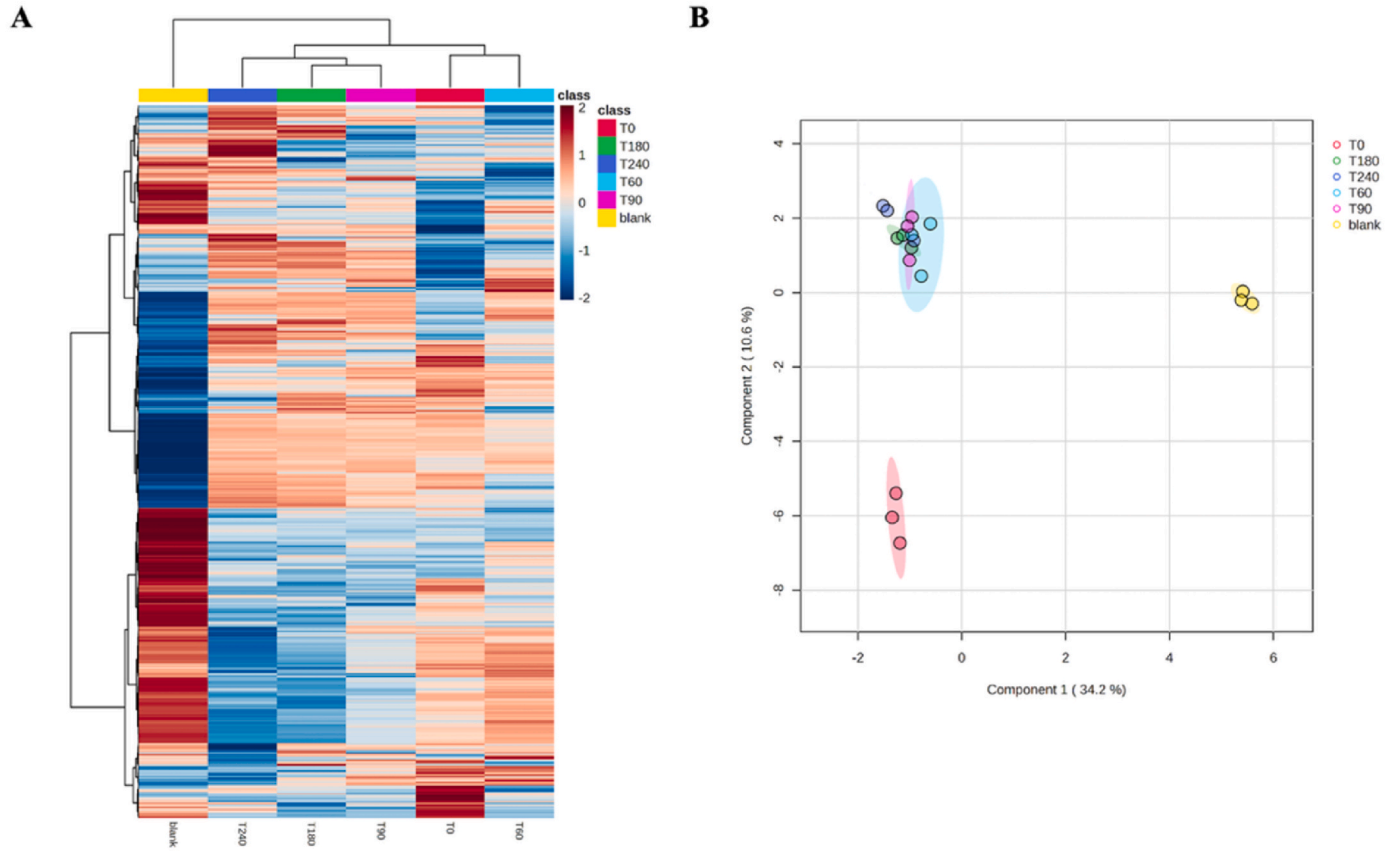

Fig. 2. Hierarchical cluster analysis (A) and sPLS-DA score plot (B) of intestinal digestates obtained after *in vitro* gastrointestinal digestion of Coppa Piacentina PDO samples at different ripening stages.

during dry-curing and ripening, such as protein aggregation, oxidation or structural rearrangements, can alter protein susceptibility to gastrointestinal enzymes by limiting the accessibility of specific cleavage sites (Paolella et al., 2015; Xiong & Guo, 2021). However, since markers of protein oxidation or cross-linking were not directly measured in the present study, these mechanisms should be regarded as plausible but not experimentally demonstrated. Overall, ripening did not enhance the release of free amino acids during *in vitro* digestion of Coppa Piacentina PDO. For a more detailed assessment, the relative distribution of individual free amino acids is reported in supplementary material. In all digested samples, lysine was the most abundant free amino acid released at the end of digestion ($P < 0.01$), accounting for 14% of total free amino acids in the 60-day ripened sample and increasing up to 23% in the 240-day ripened product. High relative abundances of glutamic acid, leucine and alanine were also consistently observed. Notably, approximately 50% of the free amino acids detected across all samples were essential amino acids, supporting the nutritional relevance of dry-cured meat products (Heres et al., 2023).

To further explore the effect of ripening extent on gastrointestinal metabolomic outcomes, supervised OPLS-DA models were constructed by grouping samples into short-ripened (60-90 days) and long-ripened (180-240 days) Coppa Piacentina PDO and comparing each group with the digested fresh product (T0). In both models, a clear discrimination between ripened and fresh digested samples was achieved along the predictive component (Fig. 3A and B), with excellent model performance ($R^2Y = 0.997$; $Q^2 = 0.870–0.878$), indicating robust and biologically meaningful separation. Additionally, the permutation test yielded significant empirical *P*-values for both R^2Y and Q^2, namely $P = 0.03$ and $P = 0.01$ for long-ripened vs T0 and short-ripened vs T0 models, respectively (supplementary material), indicating that the predictive performance of the model was statistically reliable and not affected by overfitting. The comparison between short-ripened samples and T0 revealed moderate but consistent early-stage ripening effects on proteolysis and lipid remodelling. In contrast, the long-ripened versus T0 model showed a markedly enhanced separation, indicating that prolonged ripening amplifies biochemical differences that persist after digestion. This behaviour mirrors the results obtained from data fusion analysis of the undigested product, where advanced ripening stages were associated with deeper metabolic reorganisation involving lipid oxidation, membrane remodelling and secondary reaction pathways. Therefore, ripening processes significantly modulate the intestinal metabolomic landscape rather than being neutralised during digestion.

The comparison between short-ripened Coppa Piacentina PDO (60-90 days) and the fresh product (T0) highlighted early but consistent modifications in the digestive metabolomic profile (Table 1). The VIP analysis revealed a total of 90 discriminant compounds (VIP score >0.8), of which 29 showed a significant adjusted *P*-value following FDR correction (supplementary material). Amino acids, peptides and related compounds displayed a positive cumulative Log_2FC value, indicating enhanced release of nitrogen-containing metabolites during digestion. The putative annotation of glutaminyltyrosine as the most discriminant VIP compound ($Log_2FC = 7.54$), although not significant following FDR correction (supplementary material), suggests that limited proteolysis occurring during short ripening already affects the pool of bioaccessible peptides, promoting the formation and persistence of low-molecular-weight conjugates. In parallel, fatty acids and their derivatives exhibited a moderate positive cumulative Log_2FC, with acylcarnitines such as 2-methylbutyroylcarnitine emerging as discriminant markers, but being not significantly ($P > 0.05$ following FDR correction) down-accumulated in long ripened samples ($Log_2FC = -1.42$). This finding suggests an early-stage lipid remodelling and mitochondrial-related lipid handling processes (McCann et al., 2021), in agreement with the partial membrane destabilisation observed in the data fusion analysis of the undigested product. From a nutritional perspective, some metabolites detected in the intestinal digested samples may also have relevance as dietary exposure markers. In particular, acylcarnitines, which emerged among the discriminant lipid-related metabolites, have been previously associated with red and processed meat intake in metabolomics-based nutritional studies (Wedekind et al., 2020). These compounds are involved in mitochondrial fatty acid transport and energy metabolism. Although the present *in vitro* digestion model does not allow direct extrapolation to systemic metabolic effects, their detection suggests that ripening-driven lipid remodelling may influence the pool of lipid-derived metabolites potentially available for intestinal absorption. Glycerophospholipids followed a similar positive trend (Table 1), although involving a limited number of compounds, suggesting that

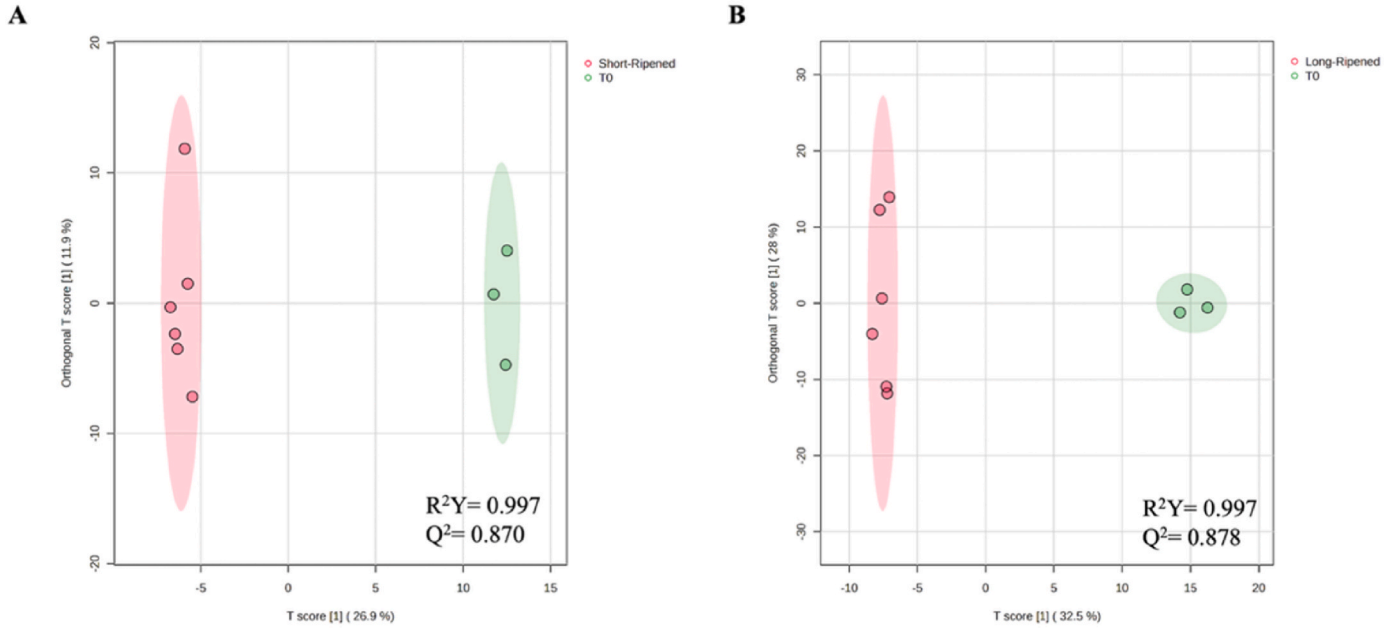

Fig. 3. OPLS-DA score plots comparing intestinal digestates of short-ripened (60–90 days) (A) and long-ripened (180–240 days) (B) Coppa Piacentina PDO with the fresh product (T0). Shaded areas represent confidence ellipses illustrating sample distribution within each group. Goodness of fitting (R^2Y) and goodness of prediction (Q^2) parameters are also reported.

Table 1
Summary of the main chemical classes discriminating short-ripened Coppa Piacentina PDO (60-90 days) from the fresh product (T0) after *in vitro* gastrointestinal digestion. For each class, the cumulative and average Log_2 fold change (Log_2FC) relative to T0 is reported together with the most discriminant compound identified by the OPLS-DA model (VIP score). The number of metabolites included in each chemical class is indicated in parentheses.

Chemical class	Short-Ripened *vs* T0	Most discriminant compound (VIP prediction model)
γ-glutamyl-peptides (n = 5)	Log_2FC (cum) = −1.87 Log_2FC (avg) = −0.37	γ-Glutamyl-Se-methylselenocysteine (VIP score = 1.401)
Amino acids, other peptides, and analogues (n = 48)	Log_2FC (cum) = 12.55 Log_2FC (avg) = 0.26	Glutaminyltyrosine (VIP score = 2.651)
Fatty acids and derivatives (n = 24)	Log_2FC (cum) = 8.67 Log_2FC (avg) = 0.36	2-Methylbutyroylcarnitine (VIP score = 1.723)
Glycerophospholipids (n = 4)	Log_2FC (cum) = 2.34 Log_2FC (avg) = 0.59	PS(16:0/18:0) (VIP score = 1.908)
Purines and pyrimidines (n = 9)	Log_2FC (cum) = 22.05 Log_2FC (avg) = 2.45	5-Methylcytosine (VIP score = 2.712)

Table 2
Summary of the main chemical classes discriminating long-ripened Coppa Piacentina PDO (180-240 days) from the fresh product (T0) after *in vitro* gastrointestinal digestion. For each class, the cumulative and average Log_2 fold change (Log_2FC) relative to T0 is reported together with the most discriminant compound identified by the OPLS-DA model (VIP score). The number of metabolites included in each chemical class is indicated in parentheses.

Chemical class	Long-Ripened *vs* T0	Most discriminant compound (VIP prediction model)
γ-glutamyl-peptides (n = 6)	Log_2FC (cum) = −2.32 Log_2FC (avg) = −0.39	N-γ-L-Glutamyl-D-alanine (VIP score = 1.313)
Amino acids, other peptides, and analogues (n = 58)	Log_2FC (cum) = 62.74 Log_2FC (avg) = 1.08	Indoleacetyl glutamine (VIP score = 2.695)
Fatty acids and derivatives (n = 36)	Log_2FC (cum) = 14.59 Log_2FC (avg) = 0.41	Linoelaidyl carnitine (VIP score = 2.337)
Glycerophospholipids (n = 24)	Log_2FC (cum) = 18.25 Log_2FC (avg) = 0.76	LysoPE (P-16:0/0:0) (VIP score = 2.251)
Purines and pyrimidines (n = 9)	Log_2FC (cum) = 16.35 Log_2FC (avg) = 1.82	Diadenosine pentaphosphate (VIP score = 2.075)
Triradylglycerols (n = 6)	Log_2FC (cum) = −6.30 Log_2FC (avg) = −1.05	TG (14:1 (9Z)/14:1 (9Z)/18:4 (6Z,9Z,12Z,15Z)) (VIP score = 1.332)

short ripening facilitates the partial release of membrane-associated lipids during digestion. Conversely, γ-glutamyl peptides showed an overall decrease compared to T0, possibly reflecting their increased susceptibility to gastrointestinal transformation at early ripening stages. Overall, short ripening induces limited structural modifications of the protein and lipid matrix, resulting in a digestive behaviour that remains largely comparable to that of the fresh product.

In contrast, long-ripened Coppa Piacentina PDO (180-240 days) exhibited a different digestive response, as indicated by substantially higher cumulative and average Log_2FC values across most chemical classes (Table 2). A total of 139 VIP discriminant compounds (VIP score >0.8) were identified, of which 35 showed a significant adjusted *P*-value following FDR correction (supplementary material). Amino acids, peptides and related compounds represented the main contributors to this shift, with indoleacetylglutamine ($Log_2FC = 8.34$; $P < 0.01$) emerging as the most discriminant and significant metabolite. While no data are available in scientific literature on indoleacetylglutamine as related with gastrointestinal digestion, indole metabolites have been extensively studied as robust indicators of cardiometabolic disease risk (Naja et al., 2025). Under our experimental conditions, this result reflects extensive ripening-driven proteolysis and the formation of complex amino acid conjugates that remain stable and bioaccessible during digestion. Fatty acids and their derivatives also showed an overall increase, with unsaturated acylcarnitines such as linoelaidyl carnitine ($Log_2FC = 12.58$) having the highest VIP score for long ripened samples. This pattern suggests advanced lipolysis and lipid oxidation processes occurring during prolonged ripening, which enhance the release of structurally modified lipid species during gastrointestinal digestion. Although not significant following FDR correction, the strong positive accumulation observed for glycerophospholipids, particularly lyso-phospholipid species (such as LysoPC(20:3 (5Z,8Z, 11Z)/0:0) and LPC(0:0/18:0, as reported in supplementary material), further supports membrane breakdown and increased digestibility of complex lipid assemblies (Domínguez et al., 2019). Conversely, triradylglycerols exhibited a decrease in long-ripened digested samples, suggesting that extensive lipolysis during ripening combined with *in vitro* digestion, reduces the availability of intact neutral lipids, shifting the digestive profile toward smaller lipid-derived metabolites (Kupikowska-Stobba et al., 2025). Although γ-glutamyl peptides showed an overall negative cumulative Log_2FC in long-ripened digested samples compared with T0 (Table 2), a compound-specific analysis highlighted a more differentiated response (supplementary material). Notably, N-γ-L-glutamyl-L-isoleucine, previously identified by the DIABLO data fusion model as a key cross-omics discriminator of ripening, and N-γ-L-glutamyl-L-methionine, showed positive Log_2FC values (i.e., 1.70 and 1.68, respectively) in the long-ripened versus T0 comparison. This finding indicates that, despite a general reduction of γ-glutamyl peptides during digestion, selected members of this class could exhibit remarkable resistance to gastrointestinal degradation. The detection of N-γ-L-glutamyl-L-isoleucine in the intestinal digested samples is noteworthy given its previously reported association with kokumi sensory attributes, exhibiting a kokumi sensation in water at concentrations around 5.0 mM (Wang et al., 2022). In the present study, the presence of this γ-glutamyl peptide in the intestinal digested samples indicates that γ-glutamyl-containing structures can be detected within the metabolomic profile generated under simulated gastrointestinal conditions. However, it should be noted that the untargeted metabolomic approach applied here does not directly quantify digestion kinetics or proteolytic resistance. Consequently, the detection of this peptide after digestion should be interpreted as a qualitative observation within the metabolomic profile, rather than as direct evidence of enzymatic resistance. From a structural perspective, γ-glutamyl peptides contain a characteristic γ-glutamyl linkage that has been discussed in food-derived peptide systems as potentially

influencing their susceptibility to enzymatic hydrolysis (Guha & Majumder, 2022). Beyond their sensory relevance, γ-glutamyl peptides have also been investigated for several biological activities, including anti-inflammatory, antioxidant, metal ion chelating, antitumor and hypoglycemic effects (Guha & Majumder, 2022). Within the scope of the present work, the identification of γ-glutamyl peptides in the digested samples highlights how ripening-associated biochemical transformations can influence the pool of peptide-derived metabolites detected after *in vitro* digestion. In this context, these compounds should be interpreted as putative digestion-derived molecular features linking the molecular signatures observed in the ripened product with the metabolomic profile generated during gastrointestinal simulation. Interestingly, several metabolites associated with the long-ripening stage showed large effect sizes (supplementary material), including N-γ-L-Glutamyl-D-alanine (d = −3.32), LysoPE (P-16:0/0:0) (d = −2.50), Indoleacetyl glutamine (d = 2.25), and Diadenosine pentaphosphate (d = 2.41), supporting the strong metabolic differentiation observed in the multivariate models. Similarly, selected metabolites associated with short ripening also displayed notable effect sizes (supplementary material), particularly 5-Methylcytosine (d = 3.41) and 2-Methylbutyroylcarnitine (d = −1.70).

Finally, the digestive metabolomic profiles revealed a conceptual contrast between metabolites associated with the fresh product and those emerging after prolonged ripening. S-adenosyl-L-methionine, a key discriminator of the undigested fresh Coppa Piacentina PDO (Fig. 1 and supplementary material), progressively lost relevance along ripening and digestion, whereas long-ripened samples were characterized by the persistence of selected peptides, such as γ-glutamyl derivatives and other di- or tri-peptides (i.e., isoleucyl-leucine, arginylphenylalanine, and Leu-Pro-Ile). This transition reflects a shift from metabolites indicative of metabolic vitality and cellular integrity toward compounds associated with technological maturation, sensory depth and digestive resilience. In this framework, SAM and γ-glutamyl peptides can be viewed as opposing molecular markers of product evolution, marking the departure from fresh muscle metabolism and the establishment of ripening-driven functional chemical signatures that shape the intestinal metabolomic landscape. Taken together, these results demonstrate that ripening time modulates not only the chemical composition of Coppa Piacentina PDO, but also the extent and nature of metabolites released during gastrointestinal digestion. While short ripening induces moderate and selective changes, prolonged ripening profoundly reshapes the digestive metabolomic landscape, amplifying the release of amino acid derivatives, lipid oxidation products and membrane-related metabolites. These digestive outcomes closely reflect the coordinated biochemical networks identified by the DIABLO-based data fusion approach, confirming that ripening-driven proteolysis and lipolysis establish a chemical architecture that directly influences gastrointestinal behaviour. Importantly, the metabolomic signatures observed here should be interpreted in terms of bioaccessibility and chemical transformations occurring during digestion, rather than direct evidence of nutritional or physiological effects. Within this framework, the increased diversity of digestion-derived metabolites reflects a broader biochemical reorganisation of the food matrix during ripening. This integrative view reinforces the concept that traditional long-ripening processes modulate digestive complexity through system-level biochemical reorganisation rather than through the simple accumulation of individual compounds.

4. Conclusions

This study provides an integrated and mechanistic interpretation of how ripening time shapes both the chemical architecture of Coppa Piacentina PDO and its gastrointestinal metabolic outcome. By combining DIABLO-based data fusion of metabolomic, lipidomic and volatilomic datasets with a standardized *in vitro* digestion model, our results indicate that ripening acts as a coordinated biochemical driver rather than as a collection of isolated compositional changes. The data fusion approach revealed tightly interconnected molecular networks governing the transition from fresh muscle metabolism to a technologically matured product, highlighting proteolysis, lipid remodelling and oxidative processes as key axes of long-term ripening. Importantly, the application of the INFOGEST protocol showed that these ripening-driven molecular organizations are not erased during digestion but are reflected in distinct intestinal metabolomic signatures. Short ripening induced moderate and selective changes in the pool of bioaccessible metabolites, whereas prolonged ripening markedly amplified digestive complexity, enhancing the release of amino acid derivatives, lipid-related metabolites and membrane-associated compounds. The persistence of specific γ-glutamyl peptides during digestion, including kokumi-active species highlighted by the data fusion analysis, further suggests that selected ripening-associated molecular features may exhibit relative resistance to gastrointestinal transformation. From a broader perspective, these findings indicate that traditional long-ripening processes may influence not only flavour development and product composition but also the chemical interface between dry-cured meats and gastrointestinal digestion. The integrative strategy adopted here moves beyond single-omics descriptions and provides a system-level framework to investigate how technological variables may shape digestive metabolite profiles and bioaccessibility patterns. However, several limitations should be considered when interpreting these results. The untargeted metabolomics workflow was performed in positive ionization mode only, which may limit the detection of certain acidic metabolites and lipid classes that are more efficiently ionized in negative mode. In addition, the chromatographic separation relied on a reversed-phase UHPLC approach, and therefore highly polar metabolites that would benefit from complementary HILIC-based separations may be underrepresented. Furthermore, the detection of γ-glutamyl peptides was based on untargeted metabolomic annotation (MSI level 2) rather than on a dedicated targeted peptidomics workflow or confirmation with authentic standards. Also, it should be noted that the present study did not directly assess structural protein modifications such as oxidation or aggregation, which may influence protein digestibility. Therefore, the observed differences in free amino acid release should be interpreted as associations with ripening stage rather than direct mechanistic evidence. Finally, the study relied on a static *in vitro* digestion model, and no functional bioassays were performed to directly link the observed metabolite shifts with biological activity or physiological responses. Further studies incorporating dynamic digestion models and/or *in vivo* approaches would be necessary to fully elucidate the metabolic and physiological impact of the observed differences. In addition, future investigations combining multi-platform metabolomics, targeted peptide validation and functional assays will therefore be valuable to further clarify the biological relevance of ripening-derived metabolites released during digestion. Despite these limitations, the present work contributes to a deeper biochemical understanding of dry-cured meat ripening and highlights the value of integrative omics approaches in characterizing traditional foods as complex and dynamically evolving biochemical systems.

CRediT authorship contribution statement

Federico Froldi: Writing – review & editing, Visualization, Methodology, Investigation, Formal analysis. **Gabriele Rocchetti:** Writing – review & editing, Writing – original draft, Visualization, Validation, Software, Methodology, Investigation, Formal analysis. **Giulia Leni:** Writing – review & editing, Investigation, Formal analysis, Data curation. **Gianluca Giuberti:** Writing – review & editing, Writing – original draft, Methodology, Investigation. **Samantha Sigolo:** Investigation, Formal analysis. **Aldo Prandini:** Writing – review & editing, Supervision, Project administration, Methodology.

Declaration of competing interest

The authors declare that they have no known competing financial interests or personal relationships that could have appeared to influence the work reported in this paper.

Acknowledgements

This work was supported by "Consorzio Salumi DOP Piacentini", Azione B. 2.3 Studio e ricerca impronte indelebili per "Coppa Piacentina".

Appendix A. Supplementary data

Supplementary data to this article can be found online at https://doi.org/10.1016/j.fbio.2026.108969.

Data availability

Data will be made available on request.

References

Becchi, P. P., Bellassi, P., Rocchetti, G., García-Pérez, G., Morelli, L., & Lucini, L. (2025). Natural creaming significantly modulates the metabolomic profile and bacterial community of raw milk: A case study on organic milk for parmigiano Reggiano PDO. *Food Bioscience, 473*, Article 143137.

Blaženović, I., Kind, T., Ji, J., & Fiehn, O. (2018). Software tools and approaches for compound identification of LC-MS/MS data in metabolomics. *Metabolites, 8*, 31.

Brodkorb, A., Egger, L., Alminger, M., Alvito, P., Assunção, R., Ballance, S., Bohn, T., Bourlieu-Lacanal, C., Boutrou, R., Carrière, F., Clemente, A., Corredig, M., Dupont, D., Dufour, C., Edwards, C., Golding, M., Karakaya, S., Kirkhus, B., Le Feunteun, S., … Recio, I. (2019). INFOGEST static in vitro simulation of gastrointestinal food digestion. *Nature Protocols, 14*(4), 991–1014.

Commission Regulation (EC) No. 1263/96 of 1 July 1996 supplementing the Annex to the Regulation (EC) no. 1107/96 on the registration of geographical indications and designations of origin under the procedure laid down in Article 17 of Regulation (EEC) No 2081/92.

Domínguez, R., Pateiro, M., Gagaoua, M., Barba, F. J., Zhang, W., & Lorenzo, J. M. (2019). A Comprehensive review on lipid oxidation in meat and meat products. *Antioxidants, 8*(10), 429.

Egger, L., Ménard, O., Delgado-Andrade, C., Alvito, P., Assunção, R., Balance, S., Barberá, R., Brodkorb, A., Cattenoz, T., Clemente, A., Comi, I., Dupont, D., Garcia-Llatas, G., Lagarda, M. J., Le Feunteun, S., JanssenDuijghuijsen, L., Karakaya, S., Lesmes, U., Mackie, A. R., et al. (2016). The harmonized INFOGEST in vitro digestion method: From knowledge to action. *Food Research International, 88*, 217–225.

Estévez, M., Geraert, P.-A., Liu, R., Delgado, J., Mercier, Y., & Zhang, W. (2020). Sulphur amino acids, muscle redox status and meat quality: More than building blocks – Invited review. *Meat Science, 163*, Article 108087.

Gallego, M., Mora, L., Hayes, M., Reig, M., & Toldrá, F. (2017). Effect of cooking and in vitro digestion on the antioxidant activity of dry-cured ham by-products. *Food Research International, 97*, 296–306.

Ghosh, T., Philtron, D., Zhang, W., Kechris, K., & Ghosh, D. (2021). Reproducibility of mass spectrometry based metabolomics data. *BMC Bioinformatics, 22*, 423.

Guha, S., & Majumder, K. (2022). Comprehensive review of γ-glutamyl peptides (γ-GPs) and their effect on inflammation concerning cardiovascular health. *Journal of Agricultural and Food Chemistry, 70*(26), 7851–7870.

Heres, A., Mora, L., & Toldrá, F. (2023). Bioactive and sensory di- and tripeptides generated during dry-curing of pork meat. *International Journal of Molecular Sciences, 24*(2), 1574.

Izquierdo-Sandoval, D., Duan, X., Fryganas, C., Portolés, T., Sancho, J. V., & Rubert, J. (2024). Untargeted metabolomics unravels distinct gut microbial metabolites derived from plant-based and animal-origin proteins using in vitro modeling. *Food Chemistry, 457*, Article 140161.

Kempf, K., Tajari, E., Baldermann, S., & Jira, W. (2025). Mass spectrometric identification of nitrite-induced modifications in heated model peptides and the cured pork matrix. *Food Chemistry, 492*, Article 145345.

Kupikowska-Stobba, B., Niu, H., Klojdová, I., Agregán, R., Lorenzo, J. M., & Kasprzak, M. (2025). Controlled lipid digestion in the development of functional and personalized foods for a tailored delivery of dietary fats. *Food Chemistry, 466*, Article 142151.

Leni, G., Rocchetti, G., Bertuzzi, T., Abate, A., Scansani, A., Froldi, F., & Prandini, A. (2024). Volatile compounds, gamma-glutamyl-peptides and free amino acids as biomarkers of long-ripened protected designation of origin Coppa Piacentina. *Food Chemistry, 440*, Article 138225.

Martín-Miguélez, J. M., Olegario, L. S., González-Mohino, A., Ventanas, S., & Delgado, J. (2024). Physicochemical, sensory, and safety evaluation of dry-cured fermented sausages and its plant-based meat analog. *LWT, 208*, Article 116704.

McCann, M. R., George De la Rosa, M. V., Rosania, G. R., & Stringer, K. A. (2021). L-Carnitine and acylcarnitines: Mitochondrial biomarkers for precision medicine. *Metabolites, 11*(1), 51.

Mediani, A., Hamezah, H. S., Jam, F. A., Mahadi, N. F., Chan, S. X. Y., Rohani, E. R., Che Lah, N. H., Azlan, U. K., Khairul Annuar, N. A., Azman, N. A. F., Bunawan, H., Sarian, M. N., Kamal, N., & Abas, F. (2022). A comprehensive review of drying meat products and the associated effects and changes. *Frontiers in Nutrition, 9*, Article 1057366.

Minekus, M., Alminger, M., Alvito, P., Ballance, S., Bohn, T., Bourlie, C., Carrière, F., Boutrou, R., Corredig, M., Dupont, D., Dufour, C., Egger, L., Golding, M., Karakaya, S., Kirkhus, B., Le Feunteun, S., Lesmes, U., Macierzanka, A., Mackie, A., et al. (2014). A standardised static in vitro digestion method suitable for food – An international consensus. *Food & Function, 5*, 1113–1124.

Mu, Y., Li, D., Deng, X., Lei, Y., Wang, Y., Wu, K., Jiang, L., Zhang, H., Zhao, C., Huang, Y., Yu, S., Liu, X., & Zhang, C. (2026). Effects of region and ripening on the physicochemical properties, microbiome, metabolome, and volatilome of Chinese dry-cured ham. *Food Chemistry X, 33*, Article 103502.

Naja, K., Anwardeen, N., Al-Shafai, M., & Elrayess, M. A. (2025). Indoleacetylglutamine pathway is a potential biomarker for cardiovascular diseases. *Biomolecules, 15*(3), 377.

Pang, Z., Lu, Y., Zhou, G., Hui, F., Xu, L., Viau, C., Spigelman, A. F., MacDonald, P. E., Wishart, D. S., Li, S., & Xia, J. (2024). MetaboAnalyst 6.0: Towards a unified platform for metabolomics data processing, analysis and interpretation. *Nucleic Acids Research, 52*, 398–406.

Paolella, S., Falavigna, C., Faccini, A., Virgili, R., Sforza, S., Dall'Asta, C., Dossena, A., & Galaverna, G. (2015). *Food Research International, 67*, 136–144.

Rocchetti, G., Leni, G., Errico, M., Sigolo, S., Lolli, V., Scansani, A., Froldi, F., Rebecchi, A., Caligiani, A., Bertuzzi, T., Lucini, L., & Prandini, A. (2025). An integrated approach based on UHPLC-HRMS, ^{1}H-NMR and sensory analysis reveals the exclusive lipid fingerprint of long-ripened protected designation of origin Coppa Piacentina. *Food Chemistry, 469*, Article 142612.

Rocchetti, G., Leni, G., Rebecchi, A., Dordoni, R., Giuberti, G., & Lucini, L. (2024). The distinctive effect of different insect powders as meat extenders in beef burgers subjected to cooking and in vitro gastrointestinal digestion. *Food Chemistry, 442*, Article 138422.

Rocchetti, G., Rebecchi, A., Dallolio, M., Braceschi, G., Domínguez, R., Dallolio, G., Trevisan, M., Lorenzo, J. M., & Lucini, L. (2021). Changes in the chemical and sensory profile of ripened Italian salami following the addition of different microbial starters. *Meat Science, 180*, Article 108584.

Rocchetti, G., Scansani, A., Leni, G., Sigolo, S., Bertuzzi, T., & Prandini, A. (2023). Untargeted metabolomics combined with sensory analysis to evaluate the chemical changes in Coppa Piacentina PDO during different ripening times. *Molecules, 28*(5), 2223.

Rocchetti, G., Zengin, G., Giuberti, G., Cervini, M., & Lucini, L. (2024). Impact of in vitro gastrointestinal digestion on the phenolic bioaccessibility and bioactive properties of insect-containing beef burgers. *Antioxidants, 13*(3), 365.

Rutigliano, M., Loizzo, P., Spadaccino, G., Trani, A., Tremonte, P., Coppola, R., Dilucia, F., Di Luccia, A., & la Gatta, B. (2023). A proteomic study of "Coppa Piacentina": A typical Italian dry-cured Salami. *Food Research International, 166*, Article 112613.

Sirtori, F., Dimauro, C., Bozzi, R., Aquilani, C., Franci, O., Calamai, L., Pezzati, A., & Pugliese, C. (2020). Evolution of volatile compounds and physical, chemical and sensory characteristics of Toscano PDO ham from fresh to dry-cured product. *European Food Research and Technology, 246*, 409–424.

Sugimoto, M., Sugawara, T., Obiya, S., Enomoto, A., Kaneko, M., Ota, S., Soga, T., & Tomita, M. (2020). Sensory properties and metabolomic profiles of dry-cured ham during the ripening process. *Food Research International, 129*, Article 108850.

Tomas, M., García-Pérez, P., Rivera-Pérez, A., Patrone, V., Giuberti, G., Lucini, L., & Capanoglu, E. (2024). The addition of polysaccharide gums to *Aronia melanocarpa* purees modulates the bioaccessibility of phenolic compounds and gut microbiota: A multiomics data fusion approach following in vitro digestion and fermentation. *Food Chemistry, 439*, Article 138231.

Tormási, J., Benes, E., Lengyel-Kónya, É., Berki, M., Horváth-Szanics, E., & Abrankó, L. (2025). Simultaneous determination of macronutrient digestibility of two model foods: Introduction of an integrated preparation method harmonized with the INFOGEST protocol. *Food Research International, 221*, Article 117297.

Tsafack, P. B., & Tsopmo, A. (2022). Effects of bioactive molecules on the concentration of biogenic amines in foods and biological systems. *Heliyon, 8*(9), Article e10456.

Tsugawa, H., Cajka, T., Kind, T., Ma, Y., Higgins, B., Ikeda, K., Kanazawa, M., VanderGheynst, J., Fiehn, O., & Arita, M. (2015). MS-DIAL: Data-independent MS/MS deconvolution for comprehensive metabolome analysis. *Nature Methods, 12*, 523–526.

Wang, H., Suo, R., Liu, X., Wang, Y., Sun, J., Liu, Y., Wang, W., & Wang, J. (2022). Kokumi γ-glutamyl peptides: Some insight into their evaluation and detection, biosynthetic pathways, contribution and changes in food processing. *Food Chemistry Advances, 1*, Article 100061.

Wedekind, R., Kiss, A., Keski-Rahkonen, P., Viallon, V., Rothwell, J. A., Cross, A., … Scalbert, A. (2020). A metabolomic study of red and processed meat intake and acylcarnitine concentrations in human urine and blood. *The American Journal of Clinical Nutrition, 112*(2), 381–388.

Xiong, Y. L., & Guo, A. (2021). Animal and plant protein oxidation: Chemical and functional property significance. *Foods, 10*(1), 40.

Xun, W., Yang, Y., Zhong, Y., Li, J., Zhou, N., Du, Y., Tang, S., Tan, J., Yang, K., Weng, C., Dong, H., Liao, G., & Wang, G. (2026). Integrated metabolomics and volatilomics reveal the impact of compound curing agents on lipid-related metabolites and

volatile compounds in Xuanwei ham. *Food Research International, 225*, Article 118081.

Yue, T., Fang, Q., Yin, J., Li, D. F., & Li, W. (2010). S-adenosylmethionine stimulates fatty acid metabolism-linked gene expression in porcine muscle satellite cells. *Molecular Biology Reports, 37*, 3143–3149.

Zhang, J., Pan, D., Zhou, G., Wang, Y., Dang, Y., He, J., Li, G., & Cao, J. (2019). The changes of the volatile compounds derived from lipid oxidation of boneless dry-cured hams during processing. *European Journal of Lipid Science and Technology, 121* (10), Article 1900135.